experienced an "extra" duplication event. This suggests that a fish-specific *HOX* cluster duplication occurred before the divergence of *Fugu* and zebrafish lineages more than 150 million years ago (*15*), but after the divergence of ray-finned and lobe-finned lineages. Goldfish, salmonids, and some other teleosts have experienced additional, more recent polyploidization events (*16*). Genomic analysis of basally branching ray-finned fish, such as sturgeons, *Amia*, or *Polypterus*, is necessary to clarify the timing of the *HOX* duplication event.

To determine whether "extra" fish *hox* clusters result from tandem duplication or chromosome duplication in fish, or cluster loss in tetrapods, we mapped zebrafish *hox* clusters; cloned, sequenced, and mapped four new genes whose orthologs are syntenic with *HOX* clusters in mammals (*dhh*, *evx1*, *eng1b*, and *gli*); and mapped four previously unmapped zebrafish genes [*dlx5*, *dlx6*, *dlx8*, and *pl10a*; see (*11*)] whose orthologs are linked to *HOX* clusters in mammals. These experiments showed that zebrafish has two copies of each *HOX* chromosome segment in mammals (Fig. 4). For example, the human and mouse *HOXB* chromosomes have six and four genes, respectively, whose apparent orthologs map on one of the two zebrafish chromosomes containing *hoxba* or *hoxbb* (Fig. 4). Each of these two chromosomes also has one copy of other duplicate genes, including *dlx7/dlx8*, *rara2a/rara2b*, and *hbae4/hbae1* (*11, 17*). We conclude that zebrafish has two copies of this mammalian chromosome segment. Because similar results were obtained for the other clusters (Fig. 4), we infer that *hox* cluster duplication in ray-finned fish occurred by whole chromosome duplication. Although we found a single *hoxd* cluster in zebrafish, mapping experiments identified the predicted duplicate chromosome segments (Fig. 4), suggesting secondary loss of one *hoxd* duplicate.

These results suggest two rounds of *HOX* chromosome duplication (probably whole genome duplication) before the divergence of ray-finned and lobe-finned fishes, and one more in ray-finned fish before the teleost radiation. Because gene duplicates often have a subset of the functions of the ancestral gene (*18*), mutations in duplicate genes may reveal essential functions that otherwise might remain hidden. For example, if a gene is essential for distinct early and late functions, a lethal mutation knocking out the early function might obscure the late function in a mutant mammal, but both functions would be evident if the two functions assort to different zebrafish gene duplicates. The conclusion that the genetic complexity of *hox* clusters in teleost fish has exceeded that of mammals for more than 100 million years calls into question the concept of a tight linkage of *HOX* cluster number and morphological complexity along the body axis. However, because teleosts are the most species-rich group of vertebrates and exhibit tremendous morphological diversity, it is tempting to speculate that the duplication event detected here may have provided gene copies that helped spur the teleost radiation.

References and Notes

1. R. Krumlauf, *Cell* **78**, 191 (1994); M. Kmita-Cunisse, F. Loosli, J. Bierne, W. Gehring, *Proc. Natl. Acad. Sci. U.S.A.* **95**, 3030 (1998); M. Kourakis *et al.*, *Dev. Biol.* **190**, 284 (1997); E. B. Lewis, *Nature* **276**, 565 (1978); S. Dickman, *Science* **275**, 1568 (1997).
2. D. Duboule and P. Dollé, *EMBO J.* **8**, 1497 (1989).
3. J. Garcia-Fernandez and P. W. H. Holland, *Nature* **370**, 563 (1994); A. Di Gregorio *et al.*, *Gene* **156**, 253 (1995).
4. P. W. H. Holland and J. Garcia-Fernandez, *Dev. Biol.* **173**, 382 (1996); A. Sharman and P. W. H. Holland, *Neth. J. Zool.* **46**, 47 (1996).
5. S. Aparicio *et al.*, *Nature Genet.* **16**, 79 (1997).
6. B. Misof and G. Wagner, *Mol. Phylogenet. Evol.* **5**, 309 (1996).
7. F. van der Hoeven, P. Sordino, N. Fraudeau, J. C. Izpisua-Belmonte, D. Duboule, *Mech. Dev.* **54**, 9 (1996); B. Misof, M. Blanco, G. Wagner, *J. Exp. Zool.* **274**, 193 (1996); V. Prince, L. Joly, M. Ekker, R. Ho, *Development* **125**, 407 (1998).
8. H. G. Eiken, P. R. Njolstad, A. Molven, A. Fjose, *Biochem. Biophys. Res. Commun.* **149**, 1165 (1987); P. Njolstad, A. Molven, I. Hordvik, J. Apold, A. Fjose, *Nucleic Acids Res.* **16**, 9097 (1988); P. R. Njolstad, A. Molven, H. G. Eiken, A. Fjose, *Gene* **73**, 33 (1989); P. R. Njolstad, A. Molven, J. Apold, A. Fjose, *EMBO J.* **9**, 515 (1990); J. A. Runstadler and T. D. Kocher, *Nucleic Acids Res.* **19**, 5434 (1991); P. Sordino, D. Duboule, T. Kondo, *Mech. Dev.* **59**, 165 (1996); V. Prince, C. Moens, C. Kimmel, R. Ho, *Development* **125**, 393 (1997).
9. DNA pools (plate pools, then row and column pools) from an arrayed zebrafish PAC library (*19*) were screened with redundant primers (Hox-F: 5′-CGNAAGAARMGNGTNCCNTAYAC-3′; Hox-R: 5′-CATNCKNCKRTTYTGRAACCANAT-3′; Hox-Fi: 5′-CTNGARYTNGARAARGARTTYCA), where N is A, C, T, or G, R is A or G, M is A or C, Y is C or T, and K is T or G. Ends of positive PACs were sequenced and specific primers used to find overlapping clones. Positive PACs were amplified with redundant primers; products were cloned and sequenced, and gene specific primers were used to obtain sequence directly from PAC DNA.
10. Unambiguously alignable sequences were obtained using CLUSTAL X (http://www-igbmc.u-strasbg.fr/BioInfo/ClustalX/Top.html) and trees were generated by the neighbor-joining method [N. Saitou and M. Nei, *Mol. Biol. Evol.* **4**, 406 (1987)]. A lamprey (*Petromyzon marinus*) cDNA library screened with redundant *hox* gene primers provided an outgroup. For accession numbers, see (*11*).
11. See *Science* Online (www.sciencemag.org) for a catalog of zebrafish *hox* genes, alignments for the phylogenetic trees in Fig. 2, accession numbers of loci used to construct the phylogenetic trees, mapping primers for zebrafish genes, and mapping data for newly mapped loci.
12. P. Ahlberg and A. Milner, *Nature* **368**, 507 (1994).
13. J. Zhang and M. Nei, *Genetics* **142**, 295 (1996); C. Kappen and F. Ruddle, *Curr. Opin. Genet. Dev.* **3**, 931 (1993).
14. W. Bailey, J. Kim, G. Wagner, F. Ruddle, *Mol. Biol. Evol.* **14**, 843 (1997); A. Meyer, *Nature* **391**, 225 (1998).
15. P. Cantatore *et al.*, *J. Mol. Evol.* **39**, 589 (1994).
16. D. G. Buth, T. Dowling, J. R. Gold, in *Cyprinid Fishes: Systematics, Biology, and Exploitation*, I. J. Winfield and J. S. Nelson, Eds. (Chapman and Hall, London, 1991), pp. 83–126; F. W. Allendorf and G. H. Thorgaard, in *Evolutionary Genetics of Fishes*, J. B. Turner, Ed. (Plenum, New York, 1984), pp. 1–53.
17. J. H. Postlethwait *et al.*, *Nature Genet.* **18**, 345 (1998).
18. S. D. Ferris and G. S. Whitt, *J. Mol. Evol.* **12**, 267 (1979); A. L. Hughes, *Proc. R. Soc. London Ser. B* **256**, 119 (1994); A. Force *et al.*, in preparation.
19. C. Amemiya, unpublished data.

20. Supported by NIH grant R01RR10715 (J.H.P.), NIH grant PHS P01HD22486 (J.H.P. and M.W.), a Medical Research Council of Canada grant (M.E.), and NSF grant IBN-9614940 (C.A.). We thank J. Miles for technical assistance.

18 June 1998; accepted 23 October 1998

Regulation of the Proinflammatory Effects of Fas Ligand (CD95L)

Jian-Jun Chen, Yongnian Sun, Gary J. Nabel*

Fas ligand (CD95L) inhibits T cell function in immune-privileged organs such as the eye and testis, yet in most tissues CD95L expression induces potent inflammatory responses. With a stably transfected colon carcinoma cell line, CT26-CD95L, the molecular basis for these divergent responses was defined. When injected subcutaneously, rejection of CT26-CD95L was caused by neutrophils activated by CD95L. CT26-CD95L survived in the intraocular space because of the presence of transforming growth factor–β (TGF-β), which inhibited neutrophil activation. Providing TGF-β to subcutaneous sites protected against tumor rejection. Thus, these cytokines together generate a microenvironment that promotes immunologic tolerance, which may aid in the amelioration of allograft rejection.

The CD95 protein (also called Fas or APO-1) is a cell surface receptor that activates the death signaling pathway in cells. Its physiological ligand, CD95L, can transduce this signal upon cell contact (*1*). The CD95-CD95L system has been implicated in the clonal deletion of autoreactive lymphocytes in peripheral lymphoid tissues and in the elimination of autoreactive lymphocyte populations (*2*), thus contributing to homeostasis

of the immune system. CD95L expression in normal tissue is restricted to T lymphocytes, macrophages, the cornea, the iris, ciliary bodies, the retina, and Sertoli cells (*3*). Through its ability to suppress both cellular and humoral immunity (*2, 4*), CD95L has been implicated in maintenance of the immune-privileged status in the eye (*3*) and testis (*5*). CD95L may also confer immune suppression in malignancy (*6*) or be useful in delaying rejection of allogeneic cells (*4, 7*) by promoting immune evasion.

However, CD95L is also proinflammatory (*8, 9*). Expression of CD95L on myotubes or pancreatic islets of transgenic mice induces a granulocytic response that accelerates graft rejection (*10*). Differences in the effect of CD95L at distinct anatomic sites may be caused by secondary factors that modulate its function (*11*). Here we attempt to identify factors that could explain the paradoxical effects of CD95L in immune-privileged sites and immunocompetent tissues.

To determine whether CD95L could stimulate an inflammatory response in an immune-privileged tissue, we injected 10^5 CT26-CD95L cells (*4*) (n = 5 mice) or a CD95L-negative control cell line, CT26-Neo (n = 4 mice), into the anterior chamber of the eye of syngeneic Balb/c mice. Both cell lines produced tumors by 8 days in all mice at the intraocular site. In contrast, tumors grew only from CT26-Neo cells when the tumor cells were injected subcutaneously (*12*). Thus, the microenvironment, rather than the amount of CD95L, determined the ability of these cells to induce inflammatory responses that inhibited tumor growth.

Rejection of CD95L$^+$ tumors occurs in *scid-beige* mice and is thus independent of T cell and natural killer (NK) cell function (*8*). Polymorphonuclear leukocytes (PMNs) infil-

Howard Hughes Medical Institute, University of Michigan Medical Center, Departments of Internal Medicine and Biological Chemistry, 1150 West Medical Center Drive, 4520 Medical Science Research Building I, Ann Arbor, MI 48109–0650, USA.

*To whom correspondence should be addressed. E-mail: gnabel@umich.edu

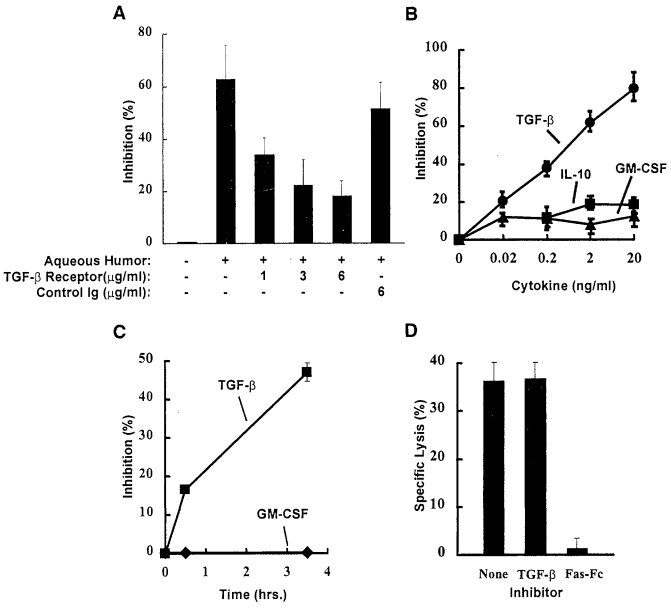

Fig. 2. Inhibitory effects of recombinant TGF-β on neutrophil-mediated cytotoxicity and its role in the aqueous humor. (**A**) Inhibitory effects of aqueous humor and reversal by neutralizing soluble TGF-β receptor protein. Mouse neutrophils were incubated with radiolabeled CT26-CD95L at a ratio of 50:1 and 40 μl of bovine aqueous humor, obtained immediately after the animal was killed and stored at −70°C. The indicated concentrations of human TGF-β–soluble receptor-Fc fusion protein (TGF-β SRII/Fc; R&D Systems) or control human immunoglobulin were added to the assay as shown in Fig. 1C. The specific lysis without inhibitor was 44.3%. (**B**) Inhibition of neutrophil cytolysis by TGF-β1. Human PMNs were incubated with CT26-CD95L cells at an E/T ratio of 100:1. Increasing amounts of human TGF-β1 (R&D Systems), human interleukin-10 (Genzyme), and granulocyte-macrophage colony-stimulating factor (GM-CSF; Immunex) were added to the culture, and Cr release assays were performed as in Fig. 1. The specific lysis without inhibitors was 44.3%. (**C**) Inhibition of neutrophil-mediated cytolysis of CT26-CD95L cells by preincubation of neutrophils with TGF-β1. Human PMNs were preincubated with TGF-β1 (20 ng/ml) or human GM-CSF (20 ng/ml) for the indicated period and washed with 10 ml of medium three times. The percent inhibition was calculated relative to neutrophils preincubated with medium, TGF-β1, or GM-CSF for the same period of time. The data represent the mean ± SE from three independent experiments. (**D**) TGF-β1 does not inhibit CD95L-mediated apoptosis in Jurkat cells. CT26-CD95L cells were incubated with ^{51}Cr-labeled Jurkat cells (1×10^4 per well) at a ratio of 10:1. Human TGF-β1 (20 ng/ml) was added to the medium, and CD95-Fc fusion protein was used as a positive control. Cytotoxicity was measured by ^{51}Cr release after 4 hours of coincubation. The data represent the mean ± SD from three independent experiments.

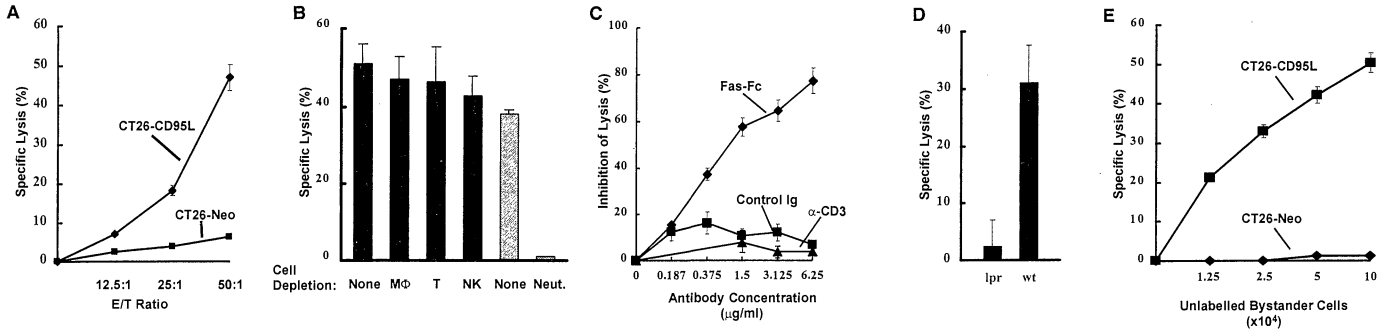

Fig. 1. PMN-mediated destruction of CD95L$^+$ CT26 cells but not CD95L$^-$ CT26 cells in vitro and CD95L involvement in neutrophil cytolytic function. (**A**) Dose-dependent cytolysis of CD95L$^+$ CT26 cells by human neutrophils. Human neutrophils (*20*) of ≥97% purity were incubated with ^{51}Cr-labeled CT26-CD95L or CT26-Neo cells for 19 hours on fibronectin-coated plates (*21*) at the indicated ratios. The data represent the mean ± SE of three independent experiments. (**B**) PMN-mediated cytolysis. Human PMNs (black bars) were depleted of T lymphocytes, NK cells, or macrophages by immunomagnetic bead separation (*22*) with antibodies to CD3, CD65, or CD115/c (Neomarkers; Pharmingen) and were mixed with CD95L$^+$ cells (50:1 ratio). Mouse neutrophils (gray bars) (*23*) were mixed with CD95L$^+$ cells (50:1 ratio). Mouse spleen cells depleted of neutrophils with antibody to Ly6G (Pharmingen) (*22*) were used as a negative control. (**C**) Inhibition of neutrophil cytotoxicity by CD95-Fc (*4*). Radiolabeled CT26-CD95L cells were mixed with neutrophils [effector/target (E/T) ratio, 50:1], and mouse CD95-Fc protein, control human immunoglobulin, or antibody to CD3 (OKT3, Ortho Biotech) was added. The specific lysis without inhibitor was 37.5%. (**D**) Lysis of CT26-CD95L by neutrophils from *lpr*$^-$/*lpr*$^-$ or wild-type congenic C57BL/6 mice at an E/T ratio of 25:1. (**E**) Induction of bystander cytotoxicity by CT26-CD95L cells. CT26-Neo target cells were labeled with ^{51}Cr and mixed with neutrophils at an E/T ratio of 100:1 in the presence of the indicated numbers of unlabeled CT26-CD95L cells. Equal numbers of unlabeled CT26-Neo cells were used as a negative control.

trate CD95L tumors in the skin and contribute to the CD95L antitumor response (*8, 9*), but the mechanism by which these cells promote tumor rejection is unknown. We therefore determined whether neutrophils could directly lyse CT26-CD95L cells in vitro. Human PMNs, incubated with CT26-CD95L or CT26-Neo target cells, lysed only CT26-CD95L (Fig. 1A). Depletion of the effector population with antibodies to T cells, NK cells, or macrophages did not reduce this cytolysis. PMNs derived from peripheral blood leukocytes of syngeneic Balb/c mice lysed CT26-CD95L tumor cells, in contrast to a control cell population depleted with a neutrophil-specific antibody, which did not retain this activity (Fig. 1B). Thus, PMNs interacted directly with $CD95L^+$ cells to mediate their destruction.

Lysis of CT26-CD95L cells was inhibited specifically by a CD95-Fc fusion protein but not by a negative control immunoglobulin (Fig. 1C) and was markedly reduced in neutrophils from *lpr* mice (Fig. 1D), which express a defective CD95 receptor. Bystander cells that did not express CD95L were lysed when chromium-labeled CT26-neo cells were incubated with unlabeled CT26-CD95L cells (Fig. 1E), which suggests that lysis of CT26-CD95L cells was not due to their intrinsic susceptibility to lysis but instead to the ability of CD95L to induce neutrophil cytotoxicity locally.

Tumors can grow intraocularly but not in subcutaneous sites. The microenvironment of the eye may contain factors, therefore, that suppress PMN activation. We tested the fluid of the anterior chamber (the aqueous humor) in cytotoxicity assays and found that it inhibited CD95L activation of PMN lytic activity (Fig. 2A). We tested several cytokines known to be present in the aqueous humor (*13*). Transforming growth factor-β1 (TGF-β1) inhibited PMN cytotoxicity in vitro (Fig. 2B), and a soluble TGF-β receptor-Fc fusion protein inhibited the suppressive effect of aqueous humor in vitro (Fig. 2A). The effect of TGF-β was on the PMNs (Fig. 2C), and the same dose of TGF-β1 had no effect on CD95L-dependent apoptosis of Jurkat cells (Fig. 2D). A similar inhibitory effect on neutrophil function was observed with human TGF-β2 (*14*).

To understand the mechanism of PMN inhibition further, we examined the activity of mitogen-activated protein kinase (MAPK) in CD95-stimulated human neutrophils. Rapid activation of p38 MAPK activity, as determined on its substrate, ATF-2 (*15*), was demonstrated in CD95L-stimulated neutrophils (Fig. 3A, lane 2). Preincubation of neutrophils with TGF-β1 suppressed this CD95L-induced activation of p38 MAPK (Fig. 3A, lane 3). Similarly to TGF-β, incubation of neutrophils with the p38 MAPK inhibitors SB203580 and SB202190 reduced neutrophil-mediated cytolysis, in contrast to a p44/42 antagonist, PD98059, that had no effect (Fig. 3B). These results demonstrated that CD95L-induced neutrophil cytotoxicity was dependent on p38 MAPK function, which is inhibited by TGF-β.

To determine whether expression of TGF-β could affect the proinflammatory effect of CD95L in subcutaneous tissue, CT26-CD95L cells were stably transfected with an expression vector encoding a constitutively active form of TGF-β1. Histologic analysis confirmed fibrosis and regression of CT26-CD95L, as reported previously (*8*), in contrast to the robust tumor growth of the double transfectants (Fig. 4A, upper panel). Occasional neutrophils were observed in the TGF-β–expressing tumors and in intraocular CT26-CD95L (Fig. 4A, lower panel), which suggests that TGF-β suppressed CD95L-induced PMN activation, although an effect on migration or survival in vivo cannot be excluded. All CT26-CD95L/TGF-β cells (n = 8) grew in recipient mice when inoculated subcutaneously, in contrast to no growth in any recipient of CT26-CD95L cells (n = 8) (Fig. 4B).

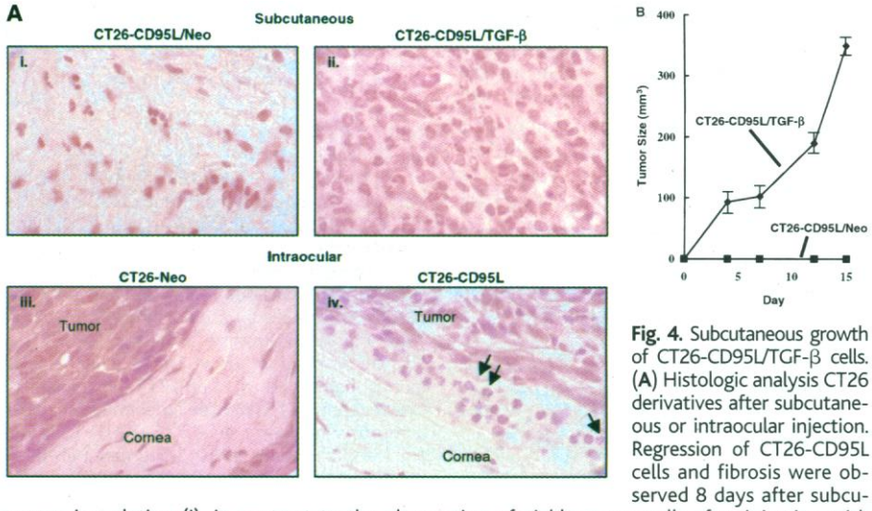

Fig. 4. Subcutaneous growth of CT26-CD95L/TGF-β cells. (**A**) Histologic analysis CT26 derivatives after subcutaneous or intraocular injection. Regression of CT26-CD95L cells and fibrosis were observed 8 days after subcutaneous inoculation (i), in contrast to the observation of viable tumor cells after injection with CT26-CD95L/TGF-β cells (ii). Tumor growth was observed intraocularly for both CT26-Neo (iii) and CT26-CD95L (iv) tumors. Arrows indicate the presence of occasional neutrophils in CT26-CD95L tumors intraocularly (iv). (**B**) Mice were injected subcutaneously with CT26-CD95L cells (n = 8) or with a subline stably transduced with a retroviral vector encoding constitutively active TGF-β1 (n = 8). Tumor volume, measured with calipers, was calculated from the largest (a) and smallest (b) diameter with the formula $0.5a \times b^2$. CT26-CD95L/TGF-β cells were generated by infection in CT26-CD95L cell line with a retrovirus vector (*24*). A constitutively active human TGF-β1 gene (*25*) was cloned into retroviral vector LZRS-pBMN-LacZ (*26*) by replacing the *lacZ* gene. TGF-β1 levels in supernatants 48 hours after infection were 8 ng/ml of TGF-β1, determined by enzyme-linked immunosorbent assay (R&D Systems). CT26-CD95L cells infected with control retroviruses (CT26-CD95L/Neo) were used as controls.

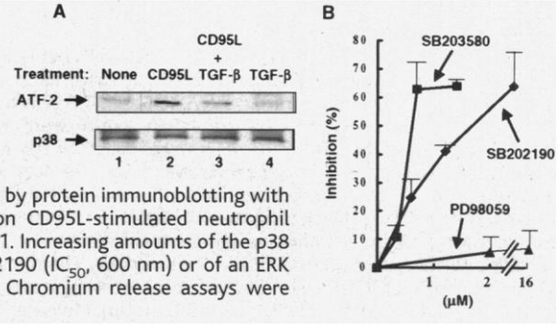

Fig. 3. p38 MAPK activation by CD95L, inhibition by TGF-β, and abrogation of CD95L-induced neutrophil cytolysis by p38 MAPK antagonists. (**A**) Activation and modulation of p38 MAPK in neutrophils by CD95L and inhibition by TGF-β. (Upper panel) Cellular p38 MAPK activity was determined by phosphorylation of an ATF2 substrate (New England Biolabs) after immunoprecipitation. Neutrophils were pretreated with human TGF-β1 (20 ng/ml, lanes 3 and 4) or with medium (lanes 1 and 2) at 4°C for 1 hour. Subsequently, the neutrophils were cocultured with human CD95L (400 ng/ml) (Upstate Biotechnology; lanes 2 and 3) or with medium (lanes 1 and 4) for 10 min at 37°C. (Lower panel) The total amount of p38 MAPK was examined by protein immunoblotting with p38 kinase antibody (New England Biolabs). (**B**) Effects of p38 MAPK inhibitors on CD95L-stimulated neutrophil cytotoxicity. Neutrophils were incubated with CT26-CD95L cells at an E/T ratio of 50:1. Increasing amounts of the p38 MAPK inhibitors SB203580 [median inhibitory concentration (IC_{50}), 350 nm] or SB202190 (IC_{50}, 600 nm) or of an ERK kinase inhibitor (negative control), PD988059 (IC_{50}, 2 μm), were added to media. Chromium release assays were performed as in Fig. 2. The specific lysis without inhibitor was 45%.

The proinflammatory effects of CD95L have raised questions about its contribution to immune privilege (*3, 5, 16*), tolerance, and graft survival (*8–10*). Although it triggers apoptosis in T lymphocytes (*2*) (Fig. 2D), CD95L unexpectedly stimulated PMN activation. As described for other PMN stimulants (*17*), this activity is dependent on its ability to enhance p38 MAPK activity (Fig. 3). PMNs directly mediate cytolysis of $CD95L^+$ cells, and this effect is inhibited by TGF-β, which is present in the aqueous humor (*13*). TGF-β also plays a role in immune tolerance through this mechanism and its effect on T cell proliferation. Although it inhibits p38 MAPK activity in other cells (*18*), its effect on innate immune responses mediated by neutrophils was previously unknown. Together CD95L and TGF-β promote lymphocyte clonal deletion and suppress inflammation. Thus, providing a microenvironment that includes both of these elements may aid in amelioration of allograft rejection at nonprivileged sites. Both CD95L and TGF-β1 have also been detected in tumors, particularly in the extracellular matrix, where they may inhibit immunologic recognition of malignancies (*6, 19*). Successful immune therapies for cancer are likely to require strategies to reverse this mechanism of immune suppression in vivo.

References and Notes

1. N. Itoh *et al.*, *Cell* **66**, 233 (1991); T. Suda, T. Takahashi, P. Golstein, S. Nagata, *ibid.* **75**, 1169 (1993).
2. T. Brunner *et al.*, *Nature* **373**, 441 (1995); J. Dhein, H. Walczak, C. Baumler, K.-M. Debatin, P. H. Krammer, *ibid.*, p. 438; S. Ju *et al.*, *ibid.*, p. 444, S. Nagata and P. Golstein, *Science* **267**, 1449 (1995).
3. T. S. Griffith, T. Brunner, S. M. Fletcher, D. R. Green, T. A. Ferguson, *Science* **270**, 1189 (1995).
4. H. Arai, S. Y. Chan, D. K. Bishop, G. J. Nabel, *Nature Med.* **3**, 843 (1997).
5. D. Bellgrau *et al.*, *Nature* **377**, 630 (1995).
6. J. O'Connell, G. C. O'Sullivan, J. K. Collins, F. Shanahan, *J. Exp. Med.* **184**, 1075 (1996); M. Hahne *et al.*, *Science* **274**, 1363 (1996); S. Strand *et al. Nature Med.* **2**, 1361 (1996).
7. H. T. Lau, M. Yu, A. Fontana, C. J. Stoeckert Jr., *Science* **273**, 109 (1996).
8. H. Arai, D. Gordon, E. G. Nabel, G. J. Nabel, *Proc. Natl. Acad. Sci. U.S.A.* **94**, 13862 (1997).
9. K.-I. Seino, N. Kayagaki, K. Okumura, H. Yagita, *Nature Med.* **3**, 165 (1997).
10. J. Allison, H. M. Georgiou, A. Strasser, D. L. Vaux, *Proc. Natl. Acad. Sci. U.S.A.* **94**, 3943 (1997); A. V. Chervonsky *et al.*, *Cell* **89**, 17 (1997); S.-M. Kang *et al.*, *Nature Med.* **3**, 738 (1997); S.-M. Kang *et al.*, *Science* **278**, 1322 (1997).
11. D. R. Green and C. F. Ware, *Proc. Natl. Acad. Sci. U.S.A.* **94**, 5986 (1997).
12. Eight-week-old female BALB/c mice from Jackson Laboratory were injected with CT26-CD95L or CT26-neo cells (10^5) in the right anterior chamber of the eye or subcutaneously into the flank after cells were harvested with trypsin, incubated in growth medium at 37°C for 1 hour, washed with phosphate-buffered saline, and resuspended in saline.
13. J. W. Streilein, G. A. Wilbanks, A. Taylor, S. Cousins, *Curr. Eye Res.* **11**, 41 (1992); M. Muhaya *et al.*, *Clin. Exp. Immunol.* **111**, 123 (1998).
14. J. J. Chen, Y. Sun, G. J. Nabel, unpublished observations.
15. J. Raingeaud *et al.*, *J. Biol. Chem.* **270**, 7420 (1995).
16. P. M. Stuart *et al.*, *J. Clin. Invest.* **99**, 396 (1997).
17. N. Nahas, T. F. Molski, G. A. Fernandez, R. I. Sha'afi, *Biochem. J.* **318**, 247 (1996); Y. L. Zu *et al.*, *J. Immunol.* **160**, 1982 (1998); J. A. Nick *et al.*, *J. Clin. Invest.* **99**, 975 (1997).
18. E. Berrou *et al.*, *Biochem. J.* **316**, 167 (1996); D. M. Rose, B. W. Winston, E. D. Chan, D. W. Riches, P. M. Henson, *Biochem. Biophys. Res. Commun.* **238**, 256 (1997); M. Lee, C. Hwang, J. Lee, H. Slavkin, D. Warburton, *Am. J. Physiol.* **273**, L374 (1998); K. Pazdrak, L. Justement, R. Alam, *J. Immunol.* **155**, 4454 (1998).
19. W. H. Daughaday and T. F. Deuel, *Endocrinol. Metab. Clin. North Am.* **20**, 539 (1991).
20. W. C. Liles, J. A. Ledbetter, A. W. Waltersdorph, S. J. Klebanoff, *J. Immunol.* **155**, 2175 (1995).
21. J. Varani *et al.*, *Am. J. Pathol.* **135**, 435 (1989); D. G. Okrent, A. K. Lichtenstein, T. Ganz, *Am. Rev. Respir. Dis.* **141**, 179 (1990).
22. K. Horgan and S. Shaw, *Curr. Protoc. Immunol.* **7**, 4 (1998).
23. Y. Luo and M. E. Dorf, *ibid.* **3**, 20 (1998).
24. Z. Yang *et al.*, *Science* **279**, 1034 (1998).
25. B. A. Arrick *et al.*, *J. Cell Biol.* **118**, 715 (1992).
26. T. M. Kinsella and G. P. Nolan, *Hum. Gene Ther.* **7**, 1405 (1996).

27. We thank D. Gschwend, N. Barrett, and L. Bentivegna for manuscript preparation; L. L. Xu for histological analysis; E. G. Nabel, M. L. Akjürek, and members of the Nabel lab for helpful advice and comments; and G. P. Nolan for providing the LZRS retroviral vector. J.J.C. is supported by the Price Fellowship and STAR program, Division of Digestive Diseases, University of California, Los Angeles.

18 May 1998; accepted 26 October 1998

Identification of Two Distinct Mechanisms of Phagocytosis Controlled by Different Rho GTPases

Emmanuelle Caron and Alan Hall*

The complement and immunoglobulin receptors are the major phagocytic receptors involved during infection. However, only immunoglobulin-dependent uptake results in a respiratory burst and an inflammatory response in macrophages. Rho guanosine triphosphatases (molecular switches that control the organization of the actin cytoskeleton) were found to be essential for both types of phagocytosis. Two distinct mechanisms of phagocytosis were identified: Type I, used by the immunoglobulin receptor, is mediated by Cdc42 and Rac, and type II, used by the complement receptor, is mediated by Rho. These results suggest a molecular basis for the different biological consequences that are associated with phagocytosis.

Phagocytosis is the process by which cells recognize and engulf large particles (>0.5 μm) and is important to host defense mechanisms as well as to tissue repair and morphogenetic remodeling. Two of the best characterized phagocytic receptors in macrophages, the complement receptor 3 (CR3) and Fc gamma receptors (FcγRs), are involved in the uptake of opsonized microorganisms during infection. CR3 binds C3bi on complement-opsonized targets, whereas FcγRs bind to immunoglobulin G (IgG)–coated targets. Phagocytosis by both types of receptors is driven by the reorganization of filamentous actin (F-actin), but the mechanisms of uptake appear to be different (*1, 2*). First, FcγR-mediated uptake is accompanied by pseudopod extension and membrane ruffling, whereas complement-opsonized targets sink into the cell, producing little protrusive activity (*3*). Second, FcγR ligation is accompanied by the activation of the respiratory burst (to produce reactive oxygen species) and by the production of arachidonic acid metabolites and cytokines, such as tumor necrosis factor–α. C3bi-dependent uptake occurs in the absence of any of these proinflammatory signals (*4–6*).

The Rho family of small guanosine triphosphatases (GTPases) is involved in the reorganization of filamentous actin structures in response to extracellular stimuli (*7*). Rho induces the assembly of contractile actomyosin filaments, whereas Rac and Cdc42 control actin polymerization into lamellipodial and filopodial membrane protrusions, respectively (*8, 9*). In addition, these GTPases can affect gene transcription [through the activation of nuclear factor kappa B, through the c-Jun NH_2-terminal kinase (JNK), and through the p38 mitogen-activated protein kinase (MAPK)], and Rac regulates the reduced form of nicotinamide adenine dinucleotide phosphate (NADPH) oxidase enzyme complex that is responsible for the respiratory burst (*10, 11*). We have, therefore, analyzed the relative roles of Rho, Rac, and Cdc42 in FcγR- and CR3-mediated phagocytosis.

Medical Research Council Laboratory for Molecular Cell Biology, Cancer Research Campaign Oncogene and Signal Transduction Group, and Department of Biochemistry, University College London, Gower Street, London WC1E 6BT, UK.

*To whom correspondence should be addressed. E-mail: alan.hall@ucl.ac.uk